Delft University of Technology

Delft Center for Systems and Control

Technical report 23-008

A novel bi-level temporally-distributed MPC approach: An application to green urban mobility*

A. Jamshidnejad, D. Sun, A. Ferrara, and B. De Schutter

Delft Center for Systems and Control
Delft University of Technology
Mekelweg 2, 2628 CD Delft
The Netherlands
phone: +31-15-278.24.73 (secretary)
URL: https://www.dcsc.tudelft.nl

---

* This report can also be downloaded via https://pub.bartdeschutter.org/abs/23_008.html

A Novel Bi-Level Temporally-Distributed MPC Approach:
An Application to Green Urban Mobility

Anahita Jamshidnejad[a,1,*], Dingshan Sun[b,1,*], Antonella Ferrara[c], Bart De Schutter[b]

[a]*Department of Control and Operations, Delft University of Technology, Kluyverweg 1, Delft, 2629 HS, The Netherlands*
[b]*Delft Center for Systems and Control, Delft University of Technology, Mekelweg 2, Delft, 2628 CD, The Netherlands*
[c]*Identification and Control of Dynamic Systems Laboratory, University of Pavia, Italy*

Abstract

Model predictive control (MPC) has been widely used for traffic management, such as for minimizing the total time spent or the total emissions of vehicles. When long-term green urban mobility is considered including e.g. a constraint on the total yearly emissions, the optimization horizon of the MPC problem is significantly larger than the control sampling time, and thus the number of the variables that should be optimized per control time step becomes very large. For systems with dynamics that involve nonlinear, non-convex, and non-smooth functions, including urban traffic networks, this results in optimization problems that are computationally intractable in real time. In this paper, we propose a novel bi-level temporal distribution of such complex MPC optimization problems, and we develop two mathematically linked short-term and long-term MPC formulations with small and large control sampling times that will be solved together instead of the original complex optimization problem. The resulting bi-level control architecture is used to solve the two MPC formulations online for real-time control of urban traffic networks with the objective of long-term green mobility. In order to assess the performance of the bi-level control architecture, we perform a case study where a rough version of the model of the urban traffic flow, S-model, is used by the long-term MPC level to estimate the states of the urban traffic networks, and a detailed version of the model is used by the short-term MPC level. The results of the simulations prove the effectiveness (with respect to the objective of control, as well as computational efficiency) of the proposed bi-level MPC approach, compared to state-of-the-art control approaches.

Keywords: Temporally distributed MPC; multiple-frequency control; green urban mobility.

1. Introduction and motivations

One of the main long-term objectives of the European Climate Law (EC, 2021) is to achieve climate neutrality by 2050, which means zero greenhouse gas emissions for all EU countries. The law, correspondingly, sets an intermediate target: to reduce the net amount of greenhouse gas emissions for, at least, 55% by 2030, compared to the levels in 1990. According to the European emissions gap report (UNEP, 2020), transportation accounts for one quarter of all the energy-related greenhouse gas emissions, and it is foreseen that by 2050 two-third of the world population will be urban. This can double the motorized mobility and lead to a 60% increase in CO_2 emissions (Outlook, 2017; Echeverría et al., 2022). Although there have been attempts to reduce the emissions by promoting the use of electric vehicles, public transit, and active transportation (e.g., walking and cycling), the traditional vehicles that exhaust emissions still make up a dominant part of the transportation. The European Environment Agency (EEA) reported in 2017 that the

amount of nitrogen dioxide produced annually across Europe had significantly violated its allowed values (EEA, 2021). Nitrogen dioxide is a main component of air pollution that is very harmful to the environment and to human health. This pollution is mostly associated with vehicle emissions, and according to EEA (2021) 86% of the nitrogen dioxide exceedances have been detected at roadside monitoring locations.

Therefore, there is an urgent need for high-performing control systems that provide green mobility by reducing the traffic emissions, especially in urban networks, which are also the focus of this paper. In order to coordinate with the climate policies, while finding a balanced trade-off between minimizing the traffic congestion and the level of harmful pollutants from the vehicle exhausts, such control systems should maintain the long-term emission levels to ensure that they do not exceed the annual emission limit.

Model predictive control (MPC) is an interesting approach for traffic control (see (Bellemans et al., 2006; Manolis et al., 2018; Wu et al., 2020; Brandi et al., 2017; Siri et al., 2021)). MPC has recently been proposed to provide green urban mobility (De Schutter, 2014; Jamshidnejad et al., 2018b, 2016)). The MPC optimization problems for green urban mobility are multi-objective and subject to several (nonlinear) control and state constraints. Thus, these problems are mathematically and computationally complex, due to the large simulation horizon

---

*Corresponding-author: Anahita Jamshidnejad and Dingshan Sun
Email addresses: `a.jamshidnejad@tudelft.nl` (Anahita Jamshidnejad), `d.sun-1@tudelft.nl` (Dingshan Sun), `Antonella.Ferrara@unipv.it` (Antonella Ferrara), `b.deschutter@tudelft.nl` (Bart De Schutter)
[1]Anahita Jamshidnejad and Dingshan Sun are co-first authors.

(i.e., weeks or months) and small control sampling time (i.e., seconds or minutes), accompanied by highly nonlinear and fluctuating dynamics of urban traffic. Next, we briefly introduce MPC and its open challenges for green urban mobility.

1.1. Model predictive control (MPC)

Model predictive control or MPC (Maciejowski, 2002; Bemporad, 2006) is a feedback-based optimal control approach. An MPC-based controller (see Figure 1 given for a discrete-time system with control sampling time c) consists of two main elements, a prediction model and an optimizer, which at every control time step run across a prediction horizon of size n^{p}. The prediction model mathematically formulates the evolution of the dynamics of the controlled system, and cooperates with the optimizer to determine a sequence of control inputs that satisfy the constraints and minimize the given cost function. The feedback-based nature of MPC, i.e., using the measured states per control time step, makes the controlled system to some extent robust to unexpected/unpredictable external disturbances (Morari and Lee, 1999). Moreover, MPC has proven to be an efficient approach for problems that should handle both input and state constraints, while optimizing multiple cost functions (Camacho and Bordons, 1995; Rawlings and Mayne, 2009).

MPC has been widely used for urban traffic signal control, and a comprehensive survey can be found in Ye et al. (2019). Tettamanti et al. (2008) is one of the early studies that utilize MPC in urban traffic management. Haddad et al. (2013) developed a macroscopic traffic modeling approach for mixed networks of freeways and arterials and solved the corresponding the optimal traffic control problem using MPC. van de Weg et al. (2018) proposed a hierarchical MPC structure considering the different dynamics in different levels of traffic networks, in which the higher layer provides reference outflow trajectories to the lower layer. Tettamanti et al. (2013) used robust MPC to develop a traffic-responsive optimal signal split algorithm taking uncertainty into account. Oliveira and Camponogara (2010) focused on the scalability of MPC for traffic signal control for large-scale traffic networks, and proposed a multi-agent MPC algorithm with graceful extension and localized reconfiguration, in which theoretical results have been investigated for the formulated linear traffic dynamic systems in terms of convergence and global optimum. However, very few studies consider the green urban mobility issue, which can introduce a long-term cumulative constraint that is difficult to be addressed by conventional MPC methods.

1.2. Current challenges of MPC for green urban mobility

The main challenges of implementing MPC for green urban mobility are explained below:

- The computational complexity of MPC can make MPC intractable in real time (Richter et al., 2012), particularly for green urban mobility where highly nonlinear dynamics, large spatial and temporal scales, and long-term control objectives and cumulative constraints are involved.
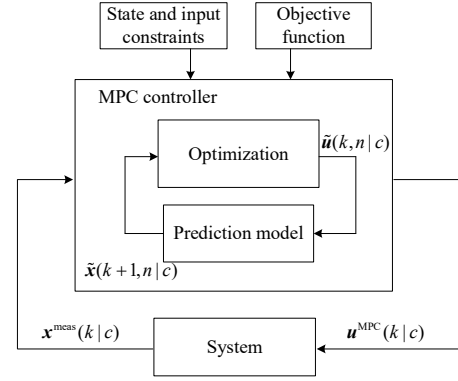

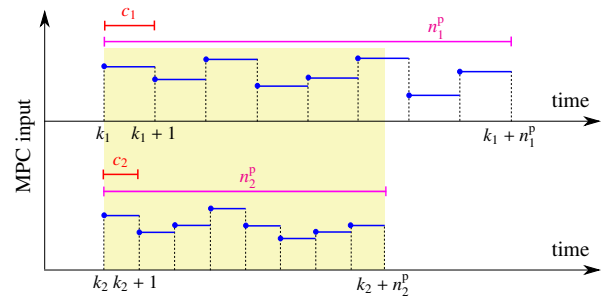Figure 1: Main structure of an MPC-based controller.

Figure 2: A decreased time scale resolution (i.e., a larger control sampling time c_1) for a larger prediction horizon n_p^1 may result in less dynamics and adaptability in the MPC input trajectory compared to when a smaller control sampling time (e.g., c_2) is considered. This is illustrated by the control inputs for the top and the bottom plot within the highlighted prediction window of length n_2^p.

- Despite providing a longer-term vision of the future (which is in benefit of the long-term control objectives and cumulative constraints), using a large prediction horizon significantly increases the computational complexity. This issue may be tackled in two ways:
    - Decreasing the time scaling resolution, i.e., using a larger control sampling time: This, however, may result in less dynamics and adaptability for the MPC input (see Fig. 2).
    - Simplifying the prediction model: This, however, may reduce the accuracy of the predicted states, and result in larger cumulative errors, particularly along a large prediction horizon.
- In general, the optimization horizon of MPC should be related to the time needed to travel through the traffic network (Aboudolas et al., 2010; Tettamanti, 2013; Kachroudi and Mammar, 2013). However, such a choice of prediction horizon cannot explicitly address long-term control objectives and cumulative constraints. This becomes particularly problematic for traffic systems that have a large time delay for the control inputs to take effects on the system.

The control frequency also matters in MPC for traffic control. A higher control frequency will improve the control per-

formance, at the price of more intensive computational complexity, while a lower control frequency requires less computational efforts, resulting however in general in a less optimal control performance. On the other hand, a larger control sampling time results in a larger prediction window (as indicated in Fig. 2), but may also lead to loss of control performance. In this paper, we reach a trade-off between accuracy and computational complexity by adopting a multi-frequency control framework, in which both a low-frequency MPC with large control sampling time and a high-frequency MPC with small control sampling time are integrated.

1.3. Contributions & structure of the paper

Therefore, in this paper, we will address the challenges of MPC for green urban mobility, to resolve the conflict between the long-term control objective and constraints on the one hand and the short-term optimization horizon on the other hand. In particular, we will propose a bi-level control architecture that embeds MPC controllers with different frequencies of operation and prediction horizons in the two control levels. The proposed control system will be implemented to an urban traffic network to achieve green mobility.

The main contributions of this paper include: 1) For the first time, a multi-level MPC-based architecture with a larger prediction horizon at the high level and a smaller prediction horizon at the low level will be implemented for obtaining green urban mobility. 2) The link and inter-dynamics of the two control levels are defined differently from any existing work: The emissions allowed in the long term are determined via the high-level MPC controller, and are adjusted for the shorter terms via the low-level MPC controller. This idea can be generalized to other fields, e.g., for energy allocation in building energy management. 3) This is the first time that MPC is adopted for long-term control of the cumulative emissions for green urban mobility. In fact, the proposed framework can limit the emissions for a long enough time span (e.g., a year), with an affordable online computation time compared to existing control methods.

Next we present a background discussion on the related theory (i.e., multi-level MPC). The rest of this paper has the following structure: Section 2 describes and formulates the MPC problem of green urban mobility. In Section 3, our proposed novel approaches for tackling complex MPC optimization problems, including that of the green urban mobility, are explained. Section 4 presents a case study, where our proposed MPC approach is compared with various state-of-the-art control methods for a simulated urban traffic network, and discusses the corresponding results. Section 5 concludes the paper and gives topics for future research. Table 1 lists and defines the frequently-used mathematical notations in the paper.

1.4. Related work

Hierarchical (multi-level) MPC schemes are often used to address complex control problem. This topic has been studied extensively, and a comprehensive review can be found in (Scattolini, 2009), where hierarchical MPC is classified into four categories:

Table 1: Frequently-used mathematical notations (using a discrete-time framework).

s	Simulation sampling time of the traffic model (e.g., 1 min). Without specification, s denotes the detailed model simulation sampling time, while s^{LT} denotes the rough model simulation sampling time
k	Without specification, k denotes the short-term MPC control time step, while k^{LT} denotes the long-term MPC control time step
c	Control sampling time: the number of time units during which a control input remains unchanged. Without specification, c denotes the short-term MPC control sampling time (e.g., 5 min), while c^{LT} denotes the long-term MPC control sampling time (e.g., 60 min)
c^{o}	Operation sampling time: every a certain number of time units the control sequence is optimized and updated. Without specification, c^{o} denotes the short-term MPC operation sampling time (e.g., 5 min), while $c^{\text{o,LT}}$ denotes the long-term MPC operation sampling time (e.g., 60 min)
$n^{\text{p}}(k)$	Prediction horizon at control time step k; in particular, $n^{\text{ST}}(k)$ denotes the short-term MPC prediction horizon, while $n^{\text{LT}}(k^{\text{LT}})$ denotes the (shrinking) long-term MPC prediction horizon
$n^{\text{s}}(k)$	Simulation horizon at control time step k, which initially equals N^{s} and shrinks gradually, where N^{s} is the considered total simulation interval length (e.g., for a simulation interval of 1 day with the simulation sampling time of 1 min, $N^{\text{s}} = 1440$)
$\boldsymbol{u}(k+\ell\|c)$	Control input at control time step $k+\ell$ (where $\ell = 0, 1, \ldots, n^{\text{p}}(k) - 1$) that is computed at control time step k, with control sampling time c (e.g., the green time length for urban traffic control). This notation applies for both short-term and long-term MPC
$\boldsymbol{x}(k+\ell\|c)$	State variable at control time step $k+\ell$ (where $\ell = 1, 2, \ldots, n^{\text{p}}(k)$) that is estimated by the prediction model at control time step k, with control sampling time c (e.g., the number of vehicles, queue lengths, vehicle speeds on each lanes, etc.). In addition, $\check{\boldsymbol{x}}$ represents the states estimated by the rough model
$\boldsymbol{x}^{\text{meas}}(k\|c)$	State variable measured at control time step k, with control sampling time c; note that $\boldsymbol{x}(k\|c) = \boldsymbol{x}^{\text{meas}}(k\|c)$
$\tilde{\boldsymbol{u}}(k,n\|c)$	Sequence of the control inputs determined at control time step k for all control time steps across the horizon n, with control sampling time c, i.e., $\tilde{\boldsymbol{u}}(k,n\|c) = [\boldsymbol{u}(k\|c), \ldots, \boldsymbol{u}(k+n-1\|c)]^{\top}$
$\tilde{\boldsymbol{x}}(k,n\|c)$	Sequence of the state variables estimated by the prediction model at control time step k for all control time steps across the horizon n, with control sampling time c, i.e., $\tilde{\boldsymbol{x}}(k,n\|c) = [\boldsymbol{x}(k+1\|c), \boldsymbol{x}(k+2\|c), \ldots, \boldsymbol{x}(k+n\|c)]^{\top}$; in addition, $\check{\tilde{\boldsymbol{x}}}$ represents the corresponding variables for the rough model
$f^{\text{state}}(\cdot)$	Detailed integrated flow-emission traffic model (e.g., an integrated macroscopic traffic model and emission model (Lin et al., 2013)); while $\check{f}^{\text{state}}(\cdot)$ denotes the extracted rough integrated model
$\bar{T}_k$	Cumulative travel time of all the vehicles at control step k. This value can be calculated via the integrated traffic model $f^{\text{state}}(\cdot)$; while $\check{\bar{T}}_{k^{\text{LT}}}(\cdot)$ represents the corresponding function for the rough model $\check{f}^{\text{state}}(\cdot)$
$\bar{E}_k$	Emissions generated at control step k. This value can be calculated via the integrated traffic model $f^{\text{state}}(\cdot)$; while $\check{\bar{E}}_{k^{\text{LT}}}(\cdot)$ represents the corresponding function for the rough model $\check{f}^{\text{state}}(\cdot)$
$\bar{V}(\cdot)$	Function computing the norm of the variation in between two consecutive control input vectors, in order to avoid significant fluctuations between the consecutive green time lengths

Note: For $\boldsymbol{u}$, $\boldsymbol{x}$, $\boldsymbol{x}^{\text{meas}}$, $\tilde{\boldsymbol{u}}$, and $\tilde{\boldsymbol{x}}$ to be complete in definition, in addition to the control sampling time, the initial control time step should generally also be given as an argument. However, we assume that the initial control time steps for all time frames, independent of the size of the control sampling time, are synchronized and coincide with a fixed, known initial time step.

1. Hierarchical MPC for coordinated control: In such architectures, a higher-level controller coordinates the control inputs generated by the lower-level local controllers, where the controllers of both levels can be MPC-based.

2. Hierarchical MPC for dealing with systems with multi-

3

ple time scales: In general, the higher-level controller operates according to slow dynamics and a lower frequency, whereas the lower-level controller operates with faster dynamics and a higher frequency. Both control levels can be used for the same system that is then described via different time scales. The high-level controller optimizes the control variables that have a long-term effect on the system, and these values are then used as references for the low-level controller to track (see, e.g., (Brdys et al., 2008; van Henten and Bontsema, 2009; van de Weg et al., 2018)). Moreover, the two control levels can be used for different sub-systems with different functionalities and control frequencies (see, e.g., (Han et al., 2021; Dunham et al., 2019)).

3. Hierarchical MPC for control of systems with a hierarchical structure: This category corresponds to a classical cascade feedback control system. For examples of controllers that belong to this category, see (Dunham et al., 2019) and (Di Cairano et al., 2019).

4. Hierarchical control for plantwide optimization: The high level of control can use the detailed dynamics of the system to compute optimal operating conditions, whereas the low level of control employs simpler dynamics to follow the references generated by the high-level controller. This control architecture is usually used in the process industry. Such a control system can also be implemented in a dual way, i.e., the high level of control uses simplified or abstracted dynamics of the system to predict the long-term performance, and considers the objective function across a large prediction horizon. Meanwhile, the low level of control works with a more accurate model and calculates the current control inputs according to a shorter prediction horizon (Pappas et al., 2000).

The following paper will be illustrated in more details, since it is more relevant to our work. Jin et al. (2019) consider the hierarchical MPC approach of category 2 to schedule the energy resources of smart buildings with a microgrid. The high level of control follows a day-ahead dynamic optimal scheduling, where the schedules of the smart buildings, distributed generators, batteries, and day-ahead setpoints of electric tie-line power are optimized for an entire day. The corresponding prediction horizon covers the duration from the current time to the end of the day, and the optimization is performed hourly. The low level of control follows an intra-hour rolling adjustment, where the low-level MPC works with a detailed model and a faster control frequency, and performs with a smaller prediction horizon. The low-level MPC tries to follow the reference (i.e., day-ahead schedules) generated by the high-level optimization process. A similar strategy is used by Liu et al. (2020) for energy management of microgrids.

Most of the literature that use hierarchical MPC consider the application in energy management for buildings, process industry, or wastewater treatment. A few researchers have also implemented hierarchical MPC for traffic management. The early work (Varaiya, 1993) proposed a four-layer control architecture for freeway traffic, where the tasks of these four layers are route choice, path planning, maneuver, and regulation. Two more recent papers (Baskar et al., 2012; Roncoli et al., 2016) employed hierarchical MPC of category 1 for coordinated control of freeway traffic networks. Su et al. (2017, 2019) consider a multi-level control strategy for the maintenance of railway networks, in which a chance-constrained MPC is used at the high level to perform a long-term optimization for the overall maintenance plan, and to provide maintenance suggestions for the low-level controllers (Su et al., 2017, 2019). Han et al. (2020) used a hierarchical control structure for the ramp metering control of a freeway network. A high-level MPC-based controller determines the optimal total inflow from the on-ramps to the freeway stretch by using an aggregated model. Then the total inflow is distributed among the on-ramps via a low-level MPC-based controller. Nonetheless, no study has considered any temporally-distributed multi-level MPC for traffic management yet. In this paper, we proposed a bi-level MPC control framework with a hierarchical structure of category 4.

2. Green urban mobility based on an annual MPC schedule

In this section, the concept of cumulative constraints for MPC is first introduced. Then we formulate the MPC problem of green urban mobility, discuss the main characteristics of the resulting optimization problem, and explain our novel approach for tackling the complexities of this problem.

2.1. Cumulative Constraints

In general, ordinary MPC only considers instantaneous constraints on the states and inputs (see the second and the third top plots in Fig. 3), which indicate, respectively, that the realized value of an equality constraint should be equal to the given value, and that the realized value of an inequality constraint should not violate the upper bound. However, cumulative constraints (i.e., constraints defined on the summation of the realized values of a variable for multiple control time steps) should be considered for green urban mobility, since there are annual emission limits required by climate policies (i.e., the cumulative emissions over the entire year should not exceed an annual limit).

For every control time step $k+1, \ldots, k+n^{\mathrm{p}}$ across the prediction horizon of MPC, the accumulated value of a specific variable (i.e., the height of the corresponding dashed bar in the top plot of Fig. 3) should not exceed a given upper bound (shown by the black continuous curve in the top plot of Fig. 3). Note that the height of each colored (blue) bar in Fig. 3 corresponds to the realized value of the variable at the current control time step. Moreover, the height of every dashed bar represents the accumulated value of this variable (i.e., the summation of the heights of the current and all the previous colored blue bars).

A main feature of cumulative constraints is that the maximum value of the corresponding variable for a given control time step (i.e., the maximum allowed height of the corresponding colored blue bar) depends on the value of the cumulative
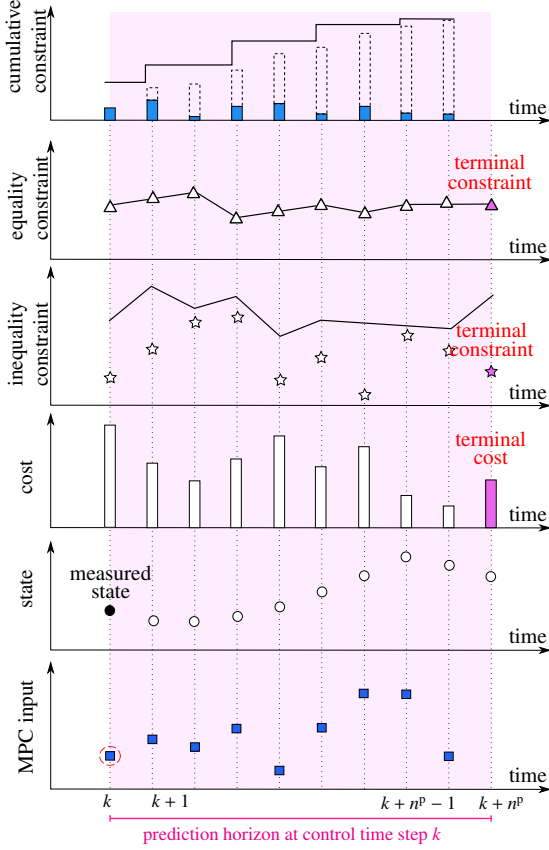
Figure 3: Illustration of the variables, cost functions, and constraints for an MPC optimization problem: In the second to fourth plots from the top, the white triangles, stars, and bars represent the stage constraints/costs and the colored triangles, stars, and bars show their terminal values. In the top plot, the dashed bars represent the realized cumulative (from control time step k until the current control time step) constraint for every control time step, whereas the colored (blue) part of the bars represent the realized value of the constraint for that particular control time step.

constraint already realized, while for instantaneous constraints the upper bound is independent of the previous values. This characteristic of cumulative constraints can provide flexibility in the predictive decision-making of MPC, i.e., by selecting an alternative optimal solution that further constrains the cumulative value at one control time step, MPC can loosen the upper bound constraint for the upcoming control time steps, and vice versa.

2.2. Problem formulation

The problem involves real-time scheduling and planning of traffic signals at the intersections of an urban traffic network, such that the congestion and total emissions of particular pollutants across a predefined simulation horizon are reduced. For the simulation horizon, we consider a fixed yearly time frame, where the control procedure begins at 0:00 of the first day of January and ends at 23:50 of the last day of December of the same year (considering a control sampling time of 10 min). The size of the simulation horizon for the entire 1 year (i.e., 365 days × 24 h × 60 min divided by the control sampling time

10 min) is given by N^s. The main constraints are on the total emissions of particular pollutants at given monitoring time steps (e.g., at the end of the year).

At control time step k (when the measured state $x^{meas}(k|c)$ is received)[2], the corresponding green mobility control problem can be formulated across the simulation horizon $n^s(k)$ (which initially equals N^s and shrinks gradually) by:

$$\min_{\tilde{u}(k,n^s(k)|c)} \left(\bar{T}_k\big(\tilde{x}(k,n^s(k)|c)\big) + \sum_{\epsilon\in\mathbb{E}} \lambda_\epsilon \bar{E}_k\big(P_\epsilon,\tilde{x}(k,n^s(k)|c)\big) + \right.$$
$$\left. \lambda^{var}\bar{V}\big(\tilde{u}(k,n^s(k)|c)\big) \right) \qquad (1)$$

s.t. :

C1: state prediction model:
$$\tilde{x}(k,n^s(k)|c) = f^{state}\big(x^{meas}(k|c),\tilde{u}(k,n^s(k)|c)\big),$$

C2: instantaneous stage and terminal constraints:
$$\tilde{x}(k,n^s(k)|c) \in \mathbb{X}^{n^s(k)}, \quad \tilde{u}(k,n^s(k)|c) \in \mathbb{U}^{n^s(k)},$$

C3: cumulative constraint $\forall \epsilon \in \mathbb{E}$:
$$\bar{E}_k(P_\epsilon,\tilde{x}(k,n^s(k)|c)) \leq \bar{E}_\epsilon^{safe} - \bar{E}_\epsilon^{real}(k|c).$$

Every control time step, the simulation horizon is reduced by 1 unit compared to the previous control time step. Thus, $n^s(k) = N^s - k$. In (1), $\bar{T}_k(\cdot)$ and $\bar{E}_k(\cdot)$ give the cumulative travel time (a quantitative measure of the traffic congestion) and the cumulative emissions of a particular pollutant for all the vehicles within the time interval corresponding to the horizon $n^s(k)$, starting at control time step k. These values can be calculated via the traffic model $f^{state}(\cdot)$ with given initial states and control inputs. Moreover, P_ϵ is a matrix that includes parameter values that are identified experimentally for every pollutant ϵ (e.g., see (Zegeye et al., 2013)) with $\mathbb{E}$ the set of all pollutants, and λ_ϵ is a weight that indicates the relative importance of various pollutants. The function $\bar{V}(\cdot)$ computes the norm of the variation in between two consecutive control input vectors and λ^{var} is the corresponding weight. In **C1**, $f^{state}(\cdot)$ is a generally nonlinear function that models the evolution of the traffic flow and emissions of the traffic network. Due to limited space, the detailed formulation of the traffic model is not presented here. The interested reader can refer to e.g. Lin et al. (2013) for more details. In **C2**, $\mathbb{X}$ and $\mathbb{U}$ are the admissible sets for the state variables and the control inputs, with the superscript $n^s(k)$ denoting the dimension. For example, the queue length should not exceed a given value to avoid backpropagation of traffic congestion, and the green time length should be within a given range. In **C3**, $\bar{E}_\epsilon^{safe}$ shows the maximum allowed value of the cumulative emissions for pollutant ϵ, which is illustrated by the continuous black curve in Fig. 3. Note that in the green urban mobility application this upper bound is fixed, i.e., it is equal to the maximal allowed annual emissions of a pollutant. Finally, $\bar{E}_\epsilon^{real}(\cdot|c)$ is the value of the total emissions of ϵ already realized by a given control time step (this value for every control time step is the height of the dashed bar at the previous time step in Fig. 3).

---

[2] We suppose that the simulation time steps coincide with the control time steps.
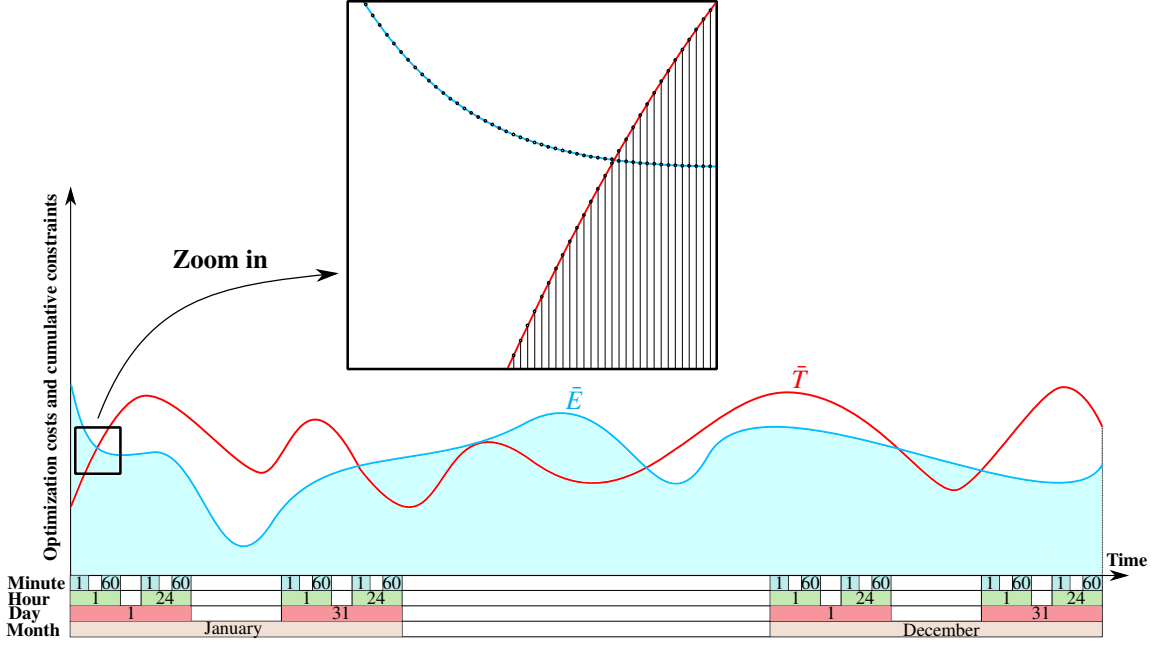
Figure 4: The significant difference between the temporal scales of the control costs (i.e., a year), cumulative constraints (i.e., up to a year), and the control input (i.e., a minute), including a zoomed-in sketch of the finest time resolution that corresponds to the control sampling time.

2.3. Characteristics of the optimization problem

The constrained optimization problem (1) has the following characteristics:

- The problem involves minimization of a cost function subject to various control and state constraints, looking into the future across a finite simulation horizon with a fixed final control time step. This implies that (1) has the structure of a shrinking-horizon optimization problem (Skaf et al., 2010).

- Due to the nonlinearities in the traffic behavior, $\bar{T}_k(\cdot)$, $\bar{E}_k(\cdot)$, and $f^{\text{state}}(\cdot)$ are in general nonlinear, non-smooth, and possibly non-convex. Therefore, (1) is generally nonlinear and non-convex.

- The green urban mobility optimization problem, including the cost function and the cumulative constraints, is defined over a relatively long time span (e.g., 12 months), while the control inputs (i.e., the green times of the traffic signals) of the controlled system (with dynamics that may be prone to rapid nonlinear changes), need to be determined at relatively high frequencies (e.g., every few seconds or minutes). These result in small control sampling times and a large value N^s for the simulation horizon, which implies a large number of optimization variables that should be determined online and in real time via (1).

- For (1) to be computationally tractable, the details may be reduced via, e.g., simplifying the prediction models and increasing the control and operation sampling times, which respectively decrease the computational burden and the number of the optimization variables. Taking these

measures may result in negative impacts on the accuracy and performance of the control system, as it was discussed in Section 1.2.

- The above-mentioned characteristics of (1), including nonlinearity, non-convexity, and long-term control objectives and constraints, next to the need for frequent online and real-time decision making, involving a large number of optimization variables, yield a complex optimization problem.

Fig. 4 illustrates the entire simulation horizon, over which the elements of the cost function, i.e., $\bar{T}_k(\cdot)$ and $\bar{E}_k(\cdot)$, and the cumulative constraints are defined. A cut of the plot (within the rectangular frame) has been zoomed in, which shows the significant difference between the temporal scales of the control input and the control costs and cumulative constraints. The characteristics of (1) mentioned earlier imply that this optimization problem may not be easy/tractable to tackle online and in real time by conventional methods. Next, we discuss how our proposed novel approaches can make (1) computationally tractable.

3. Proposed methodology for tackling the optimization complexity resulting from various temporal scales

In this section, we give our proposed approaches for tackling the complexities of (1), due to different temporal scales (i.e., small control sampling time and large simulation horizon). Our proposed methods consist of a temporal distribution and reformulation of the problem, using a shrinking-horizon approach, called *jumping-horizon*, and a bi-level multiple-frequency control architecture for implementation and solving the new formulations of the optimization problem (1).

6

3.1. Bi-level temporal distribution of the problem

In the optimization problem (1), two very different temporal scales appear, due to $N^s \gg c$. For a controlled system with a long-term cost function, an efficient control system should guarantee that the short-term control inputs will gradually lead the controlled system towards its desired long-term cost, while the short-term behavior of the controlled system also fulfills the requirements of the users of the controlled system, taking into account the rapid fluctuations of the system dynamics. Such a control system needs an overall vision of the controlled system through the entire control period, as well as more detailed information and vision about its short-term dynamics. Therefore, we propose to develop two linked MPC optimization formulations for the original optimization problem (1), where the long-term and short-term costs and constraints of (1) are distributed among these two formulations. The resulting MPC problems can be solved individually online, and their integrated solutions can result in a controlled behavior for the system that is sufficiently close to the behavior of a centralized controller that solves (1), while being significantly more computationally efficient. Next, we explain the two MPC formulations in detail.

Assumption 3.1. *It is assumed that a detailed mathematical model $f^{state}(\cdot)$ can be obtained that approximates the evolution of the traffic states and the traffic emissions accurately. Meanwhile, a rough traffic model $\check{f}^{state}(\cdot)$ can be extracted that has a larger simulation sampling time, thus resulting in long-term prediction.*

3.1.1. Rough long-term MPC formulation

A rough long-term MPC optimization problem is formulated within the same shrinking simulation window as (1), but with a (significantly) larger control sampling time c^{LT} (in this case, one-third of a month), resulting in different control time steps k^{LT}. Fig. 5 illustrates an example of the rough long-term MPC input at long-term control time step k^{LT}, assuming that k^{LT} coincides with April 1 at 0:00. Moreover, simplified versions of $\bar{T}_k(\cdot)$ and $\bar{E}_k(\cdot)$ (shown by $\check{T}_{k^{LT}}(\cdot)$ and $\check{E}_{k^{LT}}(\cdot)$), and a less detailed prediction model $\check{f}^{state}(\cdot)$ for the state variables are considered. The prediction horizon of the rough long-term MPC at long-term control time step k^{LT} is given by $n^{LT}(k^{LT})$. The initial size of the long-term prediction horizon is $N^s c/c^{LT}$, and thus for the long-term prediction horizon we have $n^{LT}(k^{LT}) = N^s c/c^{LT} - k^{LT}$. The rough long-term MPC optimization problem at long-term

control time step k^{LT} is given by:

$$
\min_{\tilde{u}(k^{LT}, n^{LT}(k^{LT})|c^{LT})} \left(\check{\bar{T}}_{k^{LT}} \left(\check{x}\left(k^{LT}, n^{LT}(k^{LT})|c^{LT}\right) \right) + \right.
$$
$$
\sum_{\epsilon \in \mathbb{E}} \lambda_\epsilon \check{\bar{E}}_{k^{LT}} \left(P_\epsilon, \check{x}\left(k^{LT}, n^{LT}(k^{LT})|c^{LT}\right) \right) +
$$
$$
\left. \lambda^{var} \bar{V} \left(\tilde{u}\left(k^{LT}, n^{LT}(k^{LT})|c^{LT}\right) \right) \right) \tag{2}
$$

s.t. :

state prediction model:
$$
\check{x}\left(k^{LT}, n^{LT}(k^{LT})|c^{LT}\right) =
$$
$$
\check{f}^{state}\left(x^{meas}\left(k^{LT}|c^{LT}\right), \tilde{u}\left(k^{LT}, n^{LT}(k^{LT})|c^{LT}\right)\right),
$$

instantaneous stage and terminal constraints:
$$
\check{x}\left(k^{LT}, n^{LT}(k^{LT})|c^{LT}\right) \in \mathbb{X}^{n^{LT}(k^{LT})},
$$
$$
\tilde{u}\left(k^{LT}, n^{LT}(k^{LT})|c^{LT}\right) \in \mathbb{U}^{n^{LT}(k^{LT})},
$$

cumulative constraint $\forall \epsilon \in \mathbb{E}$:
$$
\check{\bar{E}}_{k^{LT}}\left(P_\epsilon, \tilde{x}\left(k^{LT}, n^{LT}(k^{LT})|c^{LT}\right)\right) \leq \bar{E}_\epsilon^{safe} - \bar{E}_\epsilon^{real}(k^{LT}|c^{LT}).
$$

Note that $\check{x}$ is used to show that the corresponding states are determined by the prediction model $\check{f}^{state}(\cdot)$, instead of by $f^{state}(\cdot)$. To formulate the rough long-term MPC optimization problem (2), a good choice of c^{LT} (with $c^{LT} > c$) that results in a balanced trade-off between the time and accuracy of computations is important. This variable has been represented by a different color (red) in (2) to specify that it is a design variable in the proposed temporally-distributed approach. The solutions of the rough long-term MPC optimization problem, which are determined based on a farther vision of the future and less details in the dynamics of the controlled system, may affect the solutions of the short-term MPC optimization problem (explained next in Section 3.1.2), while they do not directly steer the controlled system.

3.1.2. Detailed short-term MPC formulation

A second MPC optimization problem is formulated across an *adaptive* prediction horizon $n^{ST}(k)$ starting at the current control time step k, with $n^{ST}(k) \leq n^s(k)$ and control sampling time c. Note that since the control sampling time of the short-term MPC formulation and (1) are the same, and also based on Remark 1, the short-term control time step is simply k. Additionally, detailed prediction models (e.g., the same as for (1)) are considered. The detailed short-term MPC optimization prob-
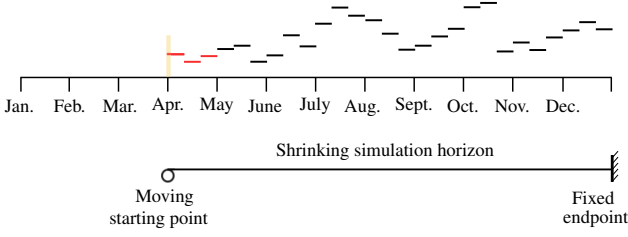
Figure 5: MPC input across the shrinking simulation horizon corresponding to the rough long-term MPC optimization formulation (c^{LT} =1/3 month).
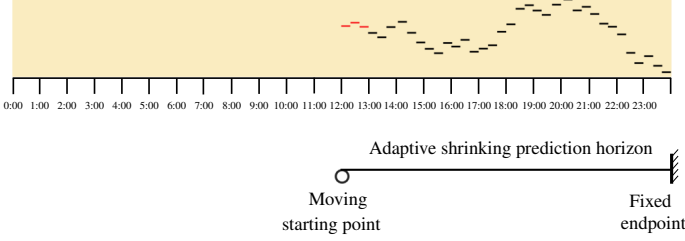

Figure 6: MPC input across the adaptive prediction horizon corresponding to the detailed short-term MPC optimization formulation for c = 20 min.

lem at control time step k is given by:

$$
\min_{\tilde{\boldsymbol{u}}\left(k, n^{\text{ST}}(k)|c\right)} \left(\bar{T}_k\left(\tilde{\boldsymbol{x}}\left(k, n^{\text{ST}}(k)|c\right)\right) + \right.
$$

$$
\sum_{\epsilon \in \mathbb{E}} \lambda_\epsilon \bar{E}_k\left(\boldsymbol{P}_\epsilon, \tilde{\boldsymbol{x}}\left(k, n^{\text{ST}}(k)|c\right)\right) +
$$

$$
\lambda^{\text{var}} \bar{V}\left(\tilde{\boldsymbol{u}}\left(k, n^{\text{ST}}(k)|c\right)\right) +
$$

$$
\lambda^{\text{term}}_{(1)}\left\|\boldsymbol{x}_{(1)}\left(k + n^{\text{ST}}(k)|c\right)\right\| - \lambda^{\text{term}}_{(2)}\left\|\boldsymbol{x}_{(2)}\left(k + n^{\text{ST}}(k)|c\right)\right\| \right) \quad (3)
$$

s.t. :

state prediction model:

$$
\tilde{\boldsymbol{x}}\left(k, n^{\text{ST}}(k)|c\right) = f^{\text{state}}\left(\boldsymbol{x}^{\text{meas}}(k|c), \tilde{\boldsymbol{u}}\left(k, n^{\text{ST}}(k)|c\right)\right),
$$

instantaneous stage and terminal constraints:

$$
\tilde{\boldsymbol{x}}\left(k, n^{\text{ST}}(k)|c\right) \in \mathbb{X}^{n^{\text{ST}}(k)}, \quad \tilde{\boldsymbol{u}}\left(k, n^{\text{ST}}(k)|c\right) \in \mathbb{U}^{n^{\text{ST}}(k)},
$$

cumulative constraint $\forall \epsilon \in \mathbb{E}$:

$$
\bar{E}_k\left(\boldsymbol{P}_\epsilon, \tilde{\boldsymbol{x}}\left(k, n^{\text{ST}}(k)|c\right)\right) \leq \bar{E}^{\text{safe, ST}}_\epsilon(k) - \bar{E}^{\text{real}}_\epsilon(k|c).
$$

At every control time step k, the short-term prediction horizon $n^{\text{ST}}(k)$ is determined and applied to the detailed short-term MPC optimization problem in a shrinking manner until the next time step $k + 1$. In (3), $\boldsymbol{x}_{(1)}$ and $\boldsymbol{x}_{(2)}$ are, respectively, the sub-vector of the state variables of $\boldsymbol{x}$ (e.g., the number of vehicles moving on the lanes and the number of vehicles idling in the queues) that should be minimized at the terminal control time step, and the sub-vector of $\boldsymbol{x}$ including the kinetic state variables (e.g., the speeds and accelerations of the vehicles) that should be maximized at the terminal control time step. The last two terms in the argument of the min function in (1) correspond to the terminal cost that is added to the short-term MPC problem, in order to compensate for the effect of reducing the size of the prediction horizon with respect to the original optimization problem. The parameters $\lambda^{\text{term}}_{(1)}$ and $\lambda^{\text{term}}_{(2)}$ are weights for the

components of the terminal cost.

Fig. 6 shows an example for the detailed short-term MPC input, where the adaptive shrinking prediction horizon starts at 0:00, has an initial size of 72, and gradually shrinks (e.g., the prediction horizon illustrated in Fig. 6 has already shrunk for 36 control time steps). Note that in this example, the detailed short-term MPC optimization problem temporally covers a part of the rough long-term MPC optimization problem that is shown within a highlighted yellow rectangle in Fig. 5 (i.e., one-tenth of the long-term control sampling time).

In formulation (3) for the detailed short-term MPC optimization problem, the choice of $n^{\text{ST}}(k)$ and $\bar{E}^{\text{safe, ST}}_\epsilon(k)$ plays an important role in the effectiveness of the determined control inputs. Therefore, we have shown these variables in color (red) to specify that these are design parameters. In general, the value of $n^{\text{ST}}(k)$ can be selected according to the size of the traffic network, such that the horizon aligns with the time needed to travel through the traffic network (Aboudolas et al., 2010; Tettamanti et al., 2013; Kachroudi and Mammar, 2013). In the proposed multi-frequency bi-level MPC framework, the high-level MPC controller can address the long-term plan with a large control sampling time and a low control frequency. Therefore, the low-level MPC can employ a normal size of prediction horizon as suggested by the references given above. The main aim of the proposed approach is to select $\bar{E}^{\text{safe, ST}}_\epsilon(k)$ in (3) based on the solution of (2), such that the resulting optimal MPC solution of (3) provides a high level of accuracy due to, both, the small control sampling time of (3) and the long-term temporal vision of (2), while a proper choice of $\bar{E}^{\text{safe, ST}}_\epsilon(\cdot)$, may result in more flexibility (i.e., less tight constraints) for the cumulative constraints in the remainder of the simulation time. Such novel integration of (2) and (3) will provide a balanced trade-off between the speed and accuracy of the optimization computations.

Remark 1. *We assume that the initial control time steps for (1), long-term, and short-term MPC optimizations overlap, and that the control sampling times of the corresponding controllers are such that the terminal control time steps for all these frameworks fall on the terminal time instant of the simulation window.*

3.1.3. Jumping-horizon MPC

We introduce the concept of *jumping-horizon MPC*, where the operation frequency of the MPC-based controller can be different from the control frequency. Operation frequency of MPC indicates how often the controller solves the optimization problem and updates the control input sequence, while control frequency implies how often the control input changes. Therefore, jumping-horizon MPC is a combination of shrinking-horizon MPC and multi-frequency MPC.

In jumping-horizon MPC, the relationship between the operation sampling time c^{o} and the control sampling time c is given by:

$$
c^{\text{o}} = \nu \cdot c, \quad \text{with} \quad 1 \leq \nu \leq n^{\text{p}}, \quad (4)
$$

where $\nu = 1$ corresponds to regular MPC explained in Section 1.1. For every control time step that coincides with an opera-
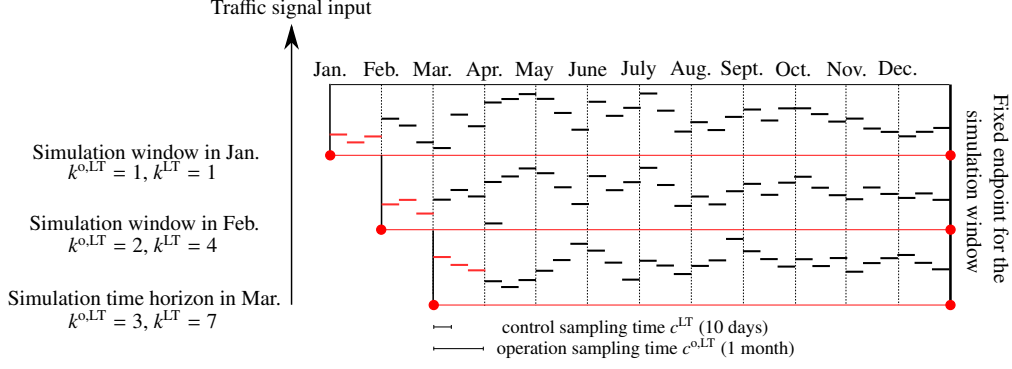
Figure 7: Jumping-horizon MPC for green urban mobility for an entire operation period of 12 months, where the frequency of operation is 3 (i.e., the controller updates the control input sequence after every 3 control time steps), the operation sampling time is 1 month, with the operation time steps coinciding with Jan., ..., Dec., and the control sampling time is one-third of a month.
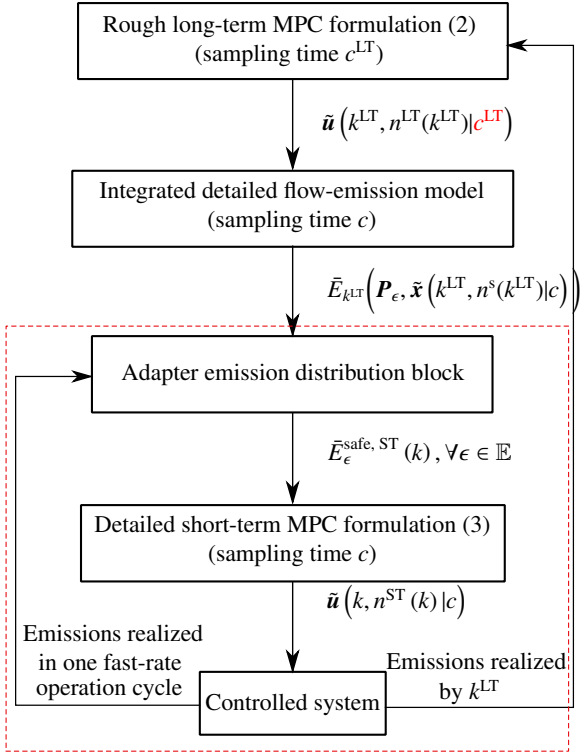

Figure 8: Linking the long-term and short-term MPC formulations at long-term control time step k^{LT} that corresponds to short-term control time step k, using an adapter block for distribution of the estimated cumulative emissions among the short-term prediction window and the remainder of the simulation window.

tion time step and the next $\nu - 1$ control time steps, the first ν elements of $\tilde{\boldsymbol{u}}(k, n^{\mathrm{p}}|c)$ are implemented to the controlled system.

Fig. 7 illustrates jumping-horizon MPC for the green mobility control problem (see Section 2) applied to the rough long-term MPC formulation. In this figure, the control sampling time is one-third of the operation sampling time, i.e., $\nu = 3$.

3.1.4. Linking the long-term and short-term MPC formulations

In order to link the long-term and short-term MPC formulations (2) and (3), we propose a bi-level control architecture with various frequencies of operation (see Fig. 8). The long-

term MPC problem (2) is solved less frequently via a *slow-rate controller*, whereas the short-term MPC problem (3) is solved via a *fast-rate controller*. In order to simplify the formulations and thus let the operation time steps overlap with the control time steps, we suppose that the operation sampling time of the slow-rate MPC controller is a multiple of the long-term control sampling time, thus a multiple of the control sampling time c (see Remark 1).

The slow-rate computations are performed via the outer loop in Fig. 8. While the slow-rate MPC controller uses a rough model for prediction, its solution $\tilde{\boldsymbol{u}}\left(k^{\mathrm{LT}}, n^{\mathrm{LT}}(k^{\mathrm{LT}})|c^{\mathrm{LT}}\right)$ is used by a detailed integrated flow-emission model (e.g., $f^{\mathrm{state}}(\cdot)$) with sampling time c to determine $\tilde{\boldsymbol{x}}\left(k^{\mathrm{LT}}, n^{\mathrm{s}}(k^{\mathrm{LT}})|c\right)$, and then $\bar{E}_{k^{\mathrm{LT}}}\left(\boldsymbol{P}_{\epsilon}, \tilde{\boldsymbol{x}}\left(k^{\mathrm{LT}}, n^{\mathrm{s}}(k^{\mathrm{LT}})|c\right)\right)$ for all $\epsilon \in \mathbb{E}$. Next, the values of the cumulative emissions estimated for the remainder of the simulation window are injected into an adapter block, which distributes these values between the current short-term prediction window (e.g., the section of the simulation window that is distinguished by a highlighted yellow rectangle in Fig. 5) and the remainder of the simulation window. The share of the cumulative emissions that is associated with the short-term prediction window by the adapter block will be used by the MPC formulation (3) as the upper bound value $\bar{E}_{\epsilon}^{\mathrm{safe, ST}}(\cdot)$ for the cumulative constraints in order to determine the control input sequences $\tilde{\boldsymbol{u}}\left(k, n^{\mathrm{ST}}(k)|c\right)$. In practice, only those elements of this control input sequence that correspond to one fast-rate operation sampling time are used to steer the system (see for instance the control inputs illustrated in red in Fig. 6) are injected into the controlled system to control the actuators (in this case the traffic signals).

After one fast-rate operation sampling time, the values of the cumulative emissions realized within this interval are sent via the controlled system to the adapter block, which uses these values to update the upper bounds for the cumulative emissions, and re-distribute these values between the current short-term window and the rest of the simulation window.

Note that the adapter block can be designed to produce in parallel various candidate distributions for the upper bound of the cumulative emissions. In that case, (3) will be solved for all

these possible distributions in parallel, and from all the optimal solutions determined, the one that corresponds to the least realized cost and/or the least value for $\bar{E}_{\epsilon}^{\text{safe, ST}}(\cdot)$ (or to the least value for a weighted combination of these two quantities) will be selected.

4. Case study

In this section, we perform two case studies with different time scales in order to evaluate the performance and validate the temporal-scalability of the proposed bi-level temporally distributed MPC approach for green mobility in an urban traffic network. The cost function consists of the total time spent (TTS) and total emissions (TE) of the vehicles traveling in the urban traffic network within a given simulation window. For the emissions, we focus on CO_2, which is the main cause of greenhouse effect. For comparison, we consider state-of-the-art control methods, including fixed-time control, responsive control, optimized fixed-time control, and conventional MPC. The performance of these controllers is assessed according to the following criteria: realized values of the total time spent by the vehicles in the urban traffic network, total emissions of CO_2, the realized value of the cost function (i.e., a weighted summation of the total time spent and total emissions, and for conventional MPC a penalty corresponding to constraint violation), as well as the CPU time for the computations of each controller.

4.1. Setup for case study 1

4.1.1. Urban traffic network

In this case study, we consider an urban traffic network (shown in Fig. 9; a similar network has been considered by Kong et al. (2013)) with 8 source/destination nodes labeled by numbers 1–8 where vehicles enter and leave the traffic network, and with 9 intersection nodes labeled by letters A–I. The arrows in the figure illustrate the links on which the vehicles can move from an upstream node to a downstream node. The numbers next to these arrows give the length of the corresponding link in m. Every two adjacent intersection nodes are connected by at least one link and at most two links with different directions. Each intersection node is controlled via a traffic signal, except for node B, which does not have a controller. A centralized controller is used for all the traffic signals, which have the same fixed cycle time equal to 1 min and are synchronous. Each directed link consists of 1-3 lanes, where the number of lanes corresponds to the number of the downstream links. As an example, the detailed illustration of a part of the urban traffic network that includes the links corresponding to nodes A and B is shown in Fig. 10. Since link (A,B) has two downstream links (B,C) and (B,E), it consists of two lanes. Vehicles that enter the traffic network via a source node are not allowed to turn immediately from the corresponding source link into a neighboring destination link and leave the traffic network (e.g., vehicles that enter via node 1 in Fig. 10 are not allowed to turn into link (A,2)). Finally, the cycle of every traffic signal includes two phases (see Fig. 11 for an intersection node with four links). Note that the same condition holds for T-shaped crosses, such as those at intersection nodes F, G, and I.
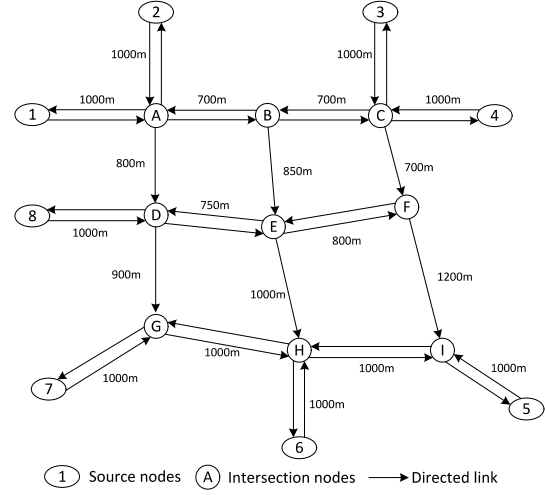

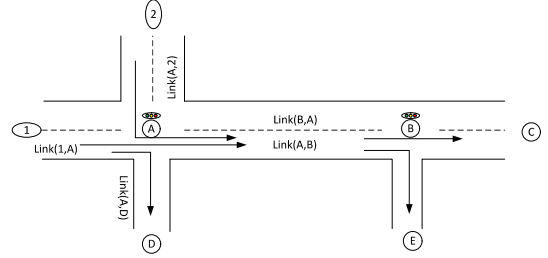Figure 9: Urban traffic network used for the case study.

Figure 10: Detailed illustration of the part of the urban traffic network that includes intersection nodes A and B.

4.1.2. Traffic flow and emission models

In this case study, the dynamics of the urban traffic flow is modeled via the S-model (Lin et al., 2011), which is macroscopic and updates the state variables of every link of the urban traffic network per simulation time step (which is considered to be equal to the cycle time of the downstream traffic signal of the link). The state variables for every link include the total number of vehicles and the number of vehicles in the queue(s) on the link (see Lin et al. (2011) and Jamshidnejad et al. (2018a) for more details). The emissions of CO_2 are calculated according to the states of the vehicles in the network, such as the acceleration and speed. More specifically, we use VT-micro (Zegeye et al., 2013) integrated with the S-model to obtain the amount of emissions (see Lin et al. (2013) for details).

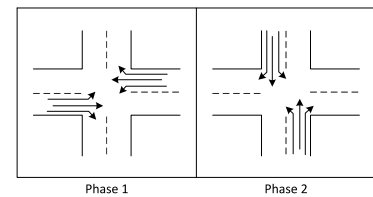For the detailed short-term and rough long-term MPC con-

Figure 11: Illustration of the two phases corresponding to the cycle of every traffic signal.

10

Table 2: Parameters of the integrated flow and emission model used for the case study

v^{free} [m/s]	v^{idle} [m/s]	a^{acc} [m/s^2]	a^{dec} [m/s^2]	l^{veh} [m]
16.67	1.11	2	-2	5

trollers, two versions of the S-model are considered: the S-model with a detailed simulation sampling time (equal to the cycle time of the traffic signals, i.e., 1 min), and the S-model with a rough simulation sampling time (five times the cycle time of the traffic signals, i.e., 5 min), respectively. The rough version of the S-model approximates the state variables of the urban traffic network faster and with a reduced, but acceptable accuracy compared to the detailed version of the S-model. The parameters used for the integrated flow and emission model for the urban traffic network are presented in Table 2, where v^{free} is the free-flow speed, v^{idle} is the idling speed, a^{acc} is the acceleration, a^{dec} is the deceleration, and l^{veh} is the average length of the vehicles in the traffic network.

4.1.3. Demand profiles

Six demand scenarios have been considered for a simulation window of 6 hours, beginning at 6:00 and ending at 12:00. This simulation window covers the morning rush hours. Although larger simulation windows can be considered to be controlled by the proposed approaches, we have considered this simulation window in order to compare the proposed control approach with more existing control methods with lower computational burden, where 6 h is large enough to represent various traffic flow and emission dynamics. The profiles for the traffic demands at the source nodes for the 6 scenarios are shown in Fig. 12. Compared to Scenario 1, Scenario 2 has a delayed peak in the morning and no peak for the demand at noon, while for Scenario 3 the peaks correspond to larger values of demand both in the morning and at noon. Moreover, Scenarios 4 and 5 have lower peak values both in the morning and at noon, while Scenario 6 has a higher morning peak than Scenario 1, but no peak occurs for this scenario at noon. In order to make the case study more realistic, we have included some noise to the demand profiles for Scenarios 2–6, which will be used to evaluate and compare the performance of various controllers. More specifically, in each of the Scenarios 2–6, we have added the noise signals defined by $N_1(t) = 10\sin(10t)$, $N_2(t) = 40\sin(t)$, $N_3(t) = 40\cos(2t+1)$, $N_4(t) = 45\cos(t+1)$, $N_5(t) = 50\sin(0.5t)$, $N_6(t) = 50\sin(1.2t + 1)$, $N_7(t) = 40\sin(1.5t + 1)$, $N_8(t) = 40\cos(1.3t + 1)$, to the demands at sources 1–8, respectively. The demand profiles that include the noise correspond to the predicted demands and imply that imperfect predictions of the real-life demand profiles may be available for the controllers.

Assumption 4.1. *It is assumed that historical data of traffic demands is available for the high-level long-term MPC controller, and that the real-time traffic demands can be estimated for the low-level short-term MPC controller.*

4.1.4. Cumulative emission constraints

The maximum allowed cumulative emissions of CO_2 are set to 70000 kg for all the scenarios, except for Scenario 4, where the maximum is 65000 kg. The reason for considering a smaller cumulative emissions of CO_2 in Scenario 4 is that there the demands are significantly lower compared to the other scenarios.

4.2. Controllers

For all the controllers considered in this case study, the control input variable is the green time length for each traffic signal, with a lower bound of 10 s and an upper bound of 50 s. The controllers that have been considered in this case study are introduced next.

4.2.1. Fixed-time controller

With the fixed-time controller, the green time lengths are not optimized, but are instead given as a fixed value of 30 s for all the controlled intersections within the entire simulation window of 6 h. This case is considered as a benchmark for all the other control approaches that are implemented in this case study.

4.2.2. Responsive controller

The responsive controller is an online adaptive traffic controller that updates the green time length of a controlled intersection at every control time step according to the traffic volume of the connecting links of that intersection. The links that include more vehicles will receive a larger green time length (see Section 2.1 of Keyvan-Ekbatani et al. (2019) for details). The control sampling time of the responsive controller is 1 min.

4.2.3. Optimization policies for adaptive control (OPAC)

OPAC is a computational strategy for real-time demand-responsive traffic signal control (Gartner, 1983). For the next control sampling time step, the controller estimates the upcoming traffic flows, and enumerates all the possible choices of green time length (which should be integer values within the allowed range of the control input variable) in order to find an optimal value for the corresponding green time length that results in the least total delay for the particular controlled intersection. Note that these estimations are performed for individual controlled intersections simultaneously (i.e., in a decentralized way). The dynamics of the links corresponding to the controlled intersection are updated via the S-model and are used to predict the future values of the state variables of these links. Note that the constraints on the emissions cannot be incorporated explicitly in an OPAC controller. The control sampling time of the OPAC controller is set to 1 min.

4.2.4. Optimized fixed-time controller

This controller is optimized off-line using a rough version of the S-model and demand Scenario 1 shown in Fig. 12. The optimization problem is solved considering a cost function that is defined as a weighted summation of the TTS and the TE within the simulation window, with a control sampling time of 60 min. A rough estimation of the total emissions within the simulation
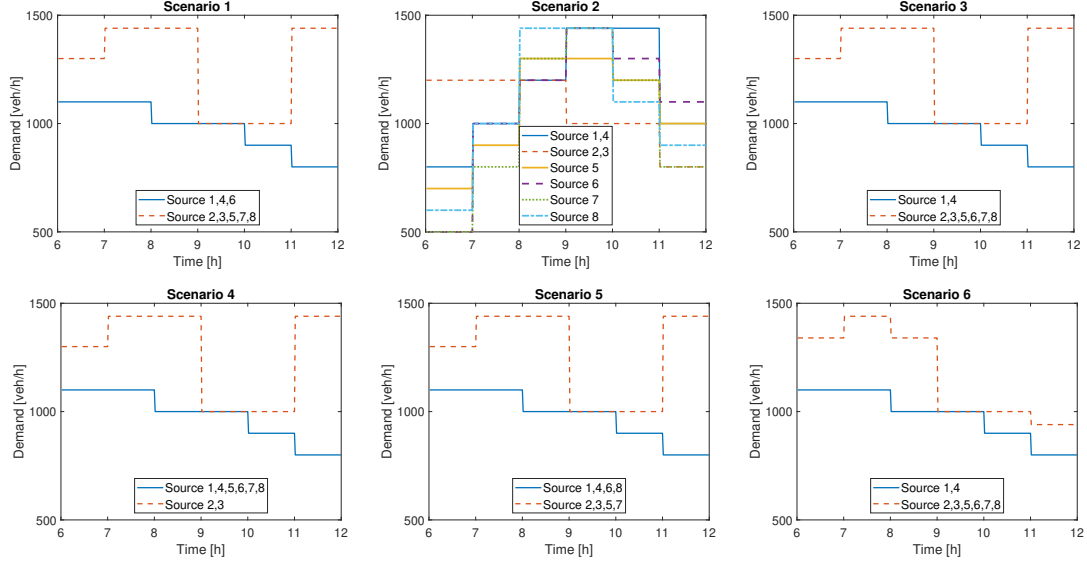
Figure 12: Demand profiles for the 6 scenarios in case study 1.

window is given as the upper bound for the cumulative constraint of the optimization problem. Whenever the optimizer fails to find a feasible solution with respect to the given constraint, the optimization problem is solved excluding the cumulative emission constraint, and a penalty corresponding to the emission constraint violation is added to the cost function. This controller is taken as the benchmark for comparison.

4.2.5. Conventional MPC controller

In order to implement an MPC controller in real time for green mobility in the given urban traffic network, the prediction time interval is limited to 15 min with a control sampling time of 5 min (i.e., the prediction horizon is 3) and an operation sampling time of 5 min. The MPC optimization problem is solved considering the detailed S-model and a cost function defined as a weighted sum of the TTS and the TE within the prediction window. The upper bound for the cumulative emissions of CO_2 within the current prediction window is estimated based on the demand profiles, i.e., the ratio of the expected demand within the current prediction window and the future expected demand is used to distribute the remaining allowed cumulative emissions. By comparing the performance and CPU time of this MPC controller and the bi-level MPC controller, we can realize how and to what extent adding the long-term MPC controller impact the overall performance of the controlled system, as well as the computational burden of the MPC controller.

4.2.6. Conventional MPC with a large prediction horizon

The same conventional MPC controller as the previous subsection, but with a larger prediction horizon is considered. The prediction time interval of this controller is doubled (i.e., it is 30 min), and therefore the prediction horizon size is 6. The other settings are exactly the same as the previous conventional MPC controller. Comparing the performance of this MPC controller with that of the bi-level and conventional MPC controller will show us whether or not we can gain the desired performance

via a single level of control, with still an affordable computation time.

4.2.7. Single-level long-term MPC controller

The rough long-term MPC-based controller in the high level of the proposed framework will be considered as the controller that directly controls the traffic network. The rough long-term MPC controller optimizes the multi-objective cost function (i.e., weighted summation of the TTS and the TE) considering a rough version of the S-model, with a simulation sampling time of 5 min, and a control and operation sampling time of 60 min. The controller originally has a prediction horizon size of 6 (equal to the simulation horizon), which is implemented in a shrinking-horizon way.

4.2.8. Bi-level temporally-distributed MPC controller

In the bi-level MPC framework the rough long-term MPC controller in the higher level of control has the same setting as the one introduced in Section 4.2.7. The parameters of the detailed short-term MPC controller in the lower level of control are similar to those of the conventional MPC controller explained in Section 4.2.5. Note that since the prediction interval of the detailed short-term MPC is 15 min, within one operation sampling time (i.e., 60 min) of the rough long-term MPC controller the short-term prediction horizon size remains 3, except for the short-term control time step corresponding to the 50th minute, for which the short-term prediction horizon size will be 2 and for the short-term control time step corresponding to the 55th minute, for which the short-term prediction horizon size will be 1. The parameter values are presented in Table 3.

For the integrated flow and emission model in the adapter block (see Fig. 8), the detailed versions of the S-model and VT-micro are used (see Lin et al. (2013) for more details). Thus, the rough control inputs determined via (2) and the predicted demands for the upcoming 1 h (see Fig. 12) are used to estimate the expected realized total emissions for the upcoming

12

Table 3: Parameters values for the case study

s	s^{LT}	$n^{\text{ST}}(k^{\text{LT}})$	$n^{\text{LT}}(k^{\text{LT}})$	c	c^{LT}	c^{o}	$c^{\text{o,LT}}$	λ_{CO_2}	λ^{var}	$\lambda^{\text{term}}_{(1)}$	$\lambda^{\text{term}}_{(2)}$
1 min	5 min	15 min	360 min	5 min	60 min	5 min	60 min	0.005	0	0	0

1 h. This value is initially distributed via the adapter block evenly among the detailed short-term control time steps. After every control time step, the upper bounds for the cumulative emissions for the remaining control time steps are updated by evenly re-distributing the value of the previous upper bound minus the value of the cumulative emissions realized in the last control sampling time. The updated upper bounds for the cumulative emissions are used by the detailed short-term MPC optimization problem to determine an optimal control input sequence that will be injected into the controlled system for the upcoming control sampling time (5 min).

Remark 2. *The proposed bi-level MPC framework can be extended to larger simulation windows, e.g., one month or one year, where additional intermediate adapter blocks can be included. For instance, one rough adapter block allocates the estimated total emissions for the entire simulation window (e.g., a month) over the individual days in the month, and a second detailed adapter block distributes these daily upper bounds over the individual hourly intervals. This approach will make the procedure computationally more efficient.*

4.3. Setup for case study 2

In this case study, a larger simulation interval (i.e., 10 days) is considered to further assess the ability of the proposed framework to fulfill the long-term control task. This case study shares the same settings as case study 1, including the urban traffic network, traffic flow and emission model, and the controllers. The only difference is the traffic demand, which extends over a longer period (see Figure 13), and the same noise is added as in Section 4.1.3. Accordingly, the rough traffic model is modified with a simulation sampling time of 2 hours. The high-level MPC controller has a control and operation sampling time of 6 hours. All the controllers introduced in case study 1 are also implemented for this case study, and their control performance is compared. Moreover, the cumulative emission constraint on CO_2 over the 10-day simulation interval is 2 million kg.

4.4. Results and Discussions

All controllers were implemented in MATLAB version R2019b running on a PC with an Intel Xeon Quad-Core E5-1620 V3 CPU with a clock speed of 3.5 GHz. Due to the nonlinear dynamics of the urban traffic network, for all the optimization-based controllers, the function `fmincon` from MATLAB has been used together with the SQP algorithm (Boggs and Tolle, 1995). Moreover, due to the non-convex nature of the optimization problems, in order to avoid selecting local optima that may result in a performance for the controller that is (much) worse than that of the global optimum, a number of off-line experiments have been conducted to determine suitable numbers of optimization starting points for achieving

near-global optima. Consequently, 10 and 15 starting points for, respectively, the rough long-term and the detailed short-term MPC optimization problems are considered. Moreover, 15 starting points are considered for the optimization problem of conventional MPC. Based on the off-line experiments, the parameters of `fmincon` were also determined such that a balance is achieved between accuracy and computational efficiency of the solver. So for the `fmincon` stopping criterion the values of the cost function tolerance, step tolerance, and constraint tolerance are selected to be 10^{-2} for the detailed short-term MPC and 10^{-1} for the rough long-term MPC. For the cost functions of (1), (2), and (3), $\lambda_{\text{CO}_2} = 0.005$ was considered, where the order of this weight corresponds to the relative orders of the total time spent of the vehicles and the total emissions of CO_2. The rest of the weights are set to 0.

Remark 3. *In case the optimization solver fails to find a feasible solution for an MPC optimization problem, it switches to another version of the problem, where the cumulative constraint on the emissions of CO_2 is excluded. A penalty is then added to the cost function with a weight equal to 0.48. This weight should be tuned carefully: with a very large value, the solver determines solutions that compromise reduction of the traffic congestion in order to decrease the total emissions of CO_2, especially for the short-term predictions, which impose short-sighted decision making. In such cases, the controller causes the vehicles to idle instead of traveling freely, since idling vehicles emit the least CO_2 per time step.*

Table 4 presents the results of the simulations for scenarios 2–6, including the CPU time and the realized values of TTS, TE, cost, and the change (in %) in the objective function (i.e., the weighted sum of the TTS and the TE) compared to the benchmark fixed-time controller for all the implemented controllers.

Overall, all controllers perform better than the fixed-time controller, while the MPC-based methods outperform the other controllers in terms of the realized values of TTS and TE, except for the single-level rough long-term MPC, which cannot guarantee the performance outside of the bi-level control architecture. For a few certain scenarios, the non-MPC methods can achieve a performance comparable to the MPC-based methods with negligible CPU time, but their performance cannot be guaranteed for all the scenarios. Furthermore, since some controllers (e.g., responsive controller and OPAC) cannot explicitly consider the constraints on the emissions, their realized TE values are much higher than those of the MPC-based methods. In addition, the bi-level MPC controller performs better than the conventional MPC, particularly in terms of the CPU time (i.e., in all cases the computational speed corresponding to the bi-level MPC controller is more than twice smaller than that of the conventional MPC controller). The bi-level MPC controller
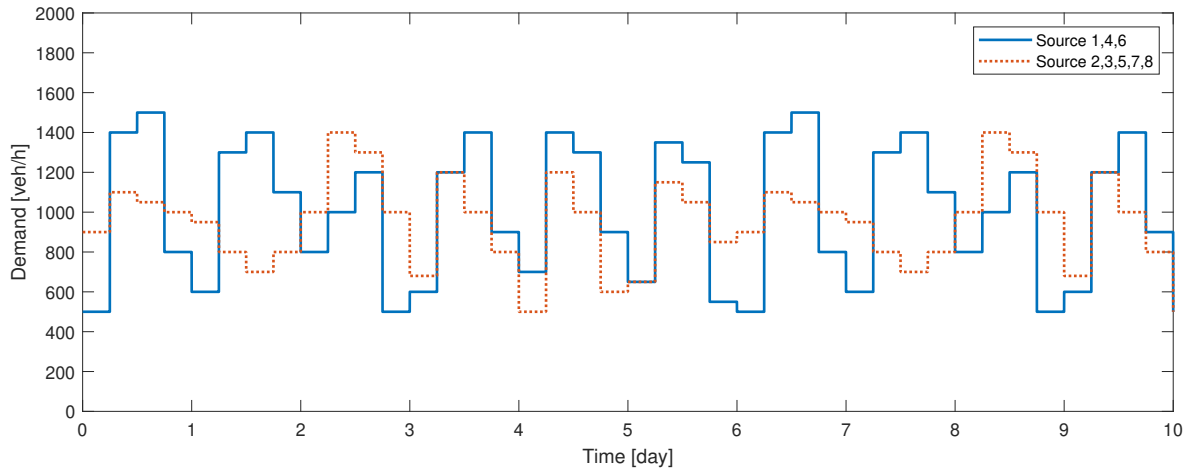
Figure 13: Demand profile for 10 days in case study 2

achieves a performance that is comparable to the large-horizon conventional MPC in terms of TTS and TE, but with significantly less CPU time. Moreover, during the simulations it was noticed that in all cases the conventional MPC controller failed to find a feasible solution under the given constraint, and hence it had to switch to the unconstrained version of the optimization problem and include a penalty term in the cost function. As a result, the computational complexity increased significantly and solutions that were obtained resulted in slightly poorer performance compared to the bi-level MPC controller. Due to the use of a higher-level rough MPC controller and the adapter block in the proposed bi-level architecture, however, the detailed short-term MPC controller most often received an upper bound for the cumulative constraint that prevented the corresponding constrained optimization problem to become infeasible.

As an extra remark, from Table 4 it is deduced that for scenario 4 the fixed-time controller performed better than all other controllers, except for the bi-level MPC-based controller. This is because the green time corresponding to the fixed-time control policy (i.e., 50% of the cycle time) is very close to the optimal solution for this scenario. Moreover, it has been verified that the MPC-based controllers result in a similar performance as the fixed-time controller. In addition, the performance of the opt. fixed-time controller cannot be guaranteed due to the quality of the historical data.

Table 5 presents the simulation results of the different controllers in case study 2. It is shown that the proposed bi-level control framework achieves the best control performance in terms of both TTS and TE, when considering a long-term green mobility control task (i.e., 10 days). In addition, the bi-level MPC framework is more computationally efficient than other MPC-based methods. This case study indicates that the proposed bi-level control framework is able to address long-term control objectives and long-term constraints that cannot be handled efficiently with conventional MPC control methods.

5. Conclusions and topics for future work

We have proposed a novel bi-level temporally-distributed MPC approach in order to tackle the challenge of high computational burden for complex constrained optimization problems with different time scales. Consequently, we have introduced two linked short-term and long-term MPC optimization problems. In the proposed framework, the rough long-term MPC problem is solved by a supervisory controller that may use a different prediction model, control sampling time, and operation time than the detailed short-term MPC problem. The controller corresponding to the detailed short-term MPC problem is implemented at the lowest control level and directly controls the system. The supervisory MPC controller determines new adaptive upper bounds for the constraints of the detailed short-term MPC problem, based on the rough long-term solutions. We have implemented the proposed control approaches to an urban traffic network in order to achieve green mobility. The results of the case study show that the proposed bi-level MPC controller outperforms other conventional control methods used for urban traffic control in terms of the total time spent, total emissions of CO_2, and CPU time. More specifically, the bi-level MPC controller has shown to require a computation time less than half of the computation time of a conventional MPC controller.

It is expected that for larger spatial and temporal scales of the network, the difference between the computation time of the bi-level MPC controller and the conventional MPC controller becomes more significant. Moreover, for future work we propose to use a more sophisticated adapter block, with several levels that distribute the upper bound of the constraints among various temporal scales. The proposed bi-level MPC architecture provides the opportunity of giving different weights to various costs in different temporal scales or for considering completely different cost functions in different temporal scales, while incorporating the inter-linked dynamics. Therefore, applying the proposed approach to various complex and non-linear dynamical systems and considering variations in the weights and costs in different temporal scales is an interesting topic for future

14

Table 4: CPU time in [s], total time spent (TTS) in [h], total emissions (TE) of CO_2 in [kg], cost, and TTS and TE compared to the benchmark fixed-time controller (in %) within the entire 6-hour simulation time window for Scenarios 2–6 of **case study 1**. For the abbreviations of the controllers: Opt. fixed-time is the optimized fixed-time controller; Conv. MPC is the conventional MPC controller; L-hori. MPC is the conventional MPC controller with a large prediction horizon; L-term MPC is the single-level long-term MPC controller. The notation '–' means that the item is not applicable to that controller. Note that the CPU time of the long-term MPC controller corresponds to a larger control sampling time than the other MPC controllers.

(a) Scenario 2

	Fixed-time	Responsive	OPAC	Opt. fixed-time	Conv. MPC	L-hori. MPC	L-term MPC	Bi-level MPC
CPU time [s]	–	–	–	–	2676	17223	269.6	1372
CPU time per control step [s]	–	–	–	–	37.17	239.2	44.93	15.06
TTS [hour]	5487.2	4815.0	4674.6	5287.2	4715.4	4675.2	5252.3	4674.9
TE(CO_2) [kg]	80232	76609	77571	79543	75484	75062	79198	75445
Objective function	5888.2	5198.0	5062.5	5684.9	5092.8	5050.5	5648.3	5052.1
Obj. value compared with Opt. fixed-time	+3.58%	-8.56%	-10.95%	–	-10.42%	-11.16%	-0.64%	-11.13%

(b) Scenario 3

	Fixed-time	Responsive	OPAC	Opt. fixed-time	Conv. MPC	L-hori. MPC	L-term MPC	Bi-level MPC
CPU time [s]	–	–	–	–	2917	22491	236.1	1608
CPU time per control step [s]	–	–	–	–	40.52	312.4	43.85	18.34
TTS [hour]	6790.3	4754.2	4603.9	4844.2	4685.1	4612.2	5185.2	4605.9
TE(CO_2) [kg]	90333	77773	78700	78245	77179	76380	80432	76745
Objective function	7242.0	5143.0	4997.4	5235.4	5071.0	4994.1	5587.4	4989.6
Obj. value compared with Opt. fixed-time	+38.33%	-1.76%	-4.55%	–	-3.14%	-4.61%	+6.72%	-4.69%

(c) Scenario 4

	Fixed-time	Responsive	OPAC	Opt. fixed-time	Conv. MPC	L-hori. MPC	L-term MPC	Bi-level MPC
CPU time [s]	–	–	–	–	3054	8956	153.4	1580
CPU time per control step [s]	–	–	–	–	42.42	124.4	25.57	17.50
TTS [hour]	4058.7	4081.2	4058.9	4399.4	4067.7	4058.7	4058.7	4058.7
TE(CO_2) [kg]	67612	67728	69990	68085	67395	67612	67612	67400
Objective function	4396.8	4419.8	4408.8	4739.8	4404.7	4396.7	4396.7	4395.7
Obj. value compared with Opt. fixed-time	-7.24%	-6.75%	-6.98%	–	-7.07%	-7.24%	-7.24%	-7.26%

(d) Scenario 5

	Fixed-time	Responsive	OPAC	Opt. fixed-time	Conv. MPC	L-hori. MPC	L-term MPC	Bi-level MPC
CPU time [s]	–	–	–	–	2990	12736	339.2	1598
CPU time per control step [s]	–	–	–	–	41.53	176.9	56.5	17.94
TTS [hour]	4426.2	4389.9	4329.4	4329.5	4352.1	4334.4	4330.4	4329.2
TE(CO_2) [kg]	72783	72445	74152	72482	71919	71638	71840	71858
Objective function	4790.1	4752.1	4700.2	4691.9	4711.7	4692.6	4689.6	4688.5
Obj. value compared with Opt. fixed-time	+2.09%	+1.28%	+0.18%	–	+0.42%	0.00%	0.00%	0.00%

(e) Scenario 6

	Fixed-time	Responsive	OPAC	Opt. fixed-time	Conv. MPC	L-hori. MPC	L-term MPC	Bi-level MPC
CPU time [s]	–	–	–	–	3114	18771	254	1577
CPU time per control step [s]	–	–	–	–	43.26	260.7	42.3	18.63
TTS [hour]	6686.7	4889.9	4722.6	4734.7	4760.6	4722.2	4975.2	4730.3
TE(CO_2) [kg]	88708	77811	78769	77120	76610	76231.4	78390	76602
Objective function	7130.2	5279.0	5116.4	5120.3	5143.6	5103.4	5367.1	5113.3
Obj. value compared with Opt. fixed-time	+39.25%	+3.10%	0.00%	–	+0.46%	-0.33%	+4.82%	-0.14%

work.

References

Aboudolas, K., Papageorgiou, M., Kouvelas, A., Kosmatopoulos, E., 2010. A rolling-horizon quadratic-programming approach to the signal control problem in large-scale congested urban road networks. Transportation Research Part C: Emerging Technologies 18, 680–694.

Baskar, L.D., De Schutter, B., Hellendoorn, H., 2012. Traffic management for automated highway systems using model-based predictive control. IEEE Transactions on Intelligent Transportation Systems 13, 838–847.

Bellemans, T., De Schutter, B., De Moor, B., 2006. Model predictive control for ramp metering of motorway traffic: A case study. Control Engineering Practice 14, 757–767.

Bemporad, A., 2006. Model predictive control design: New trends and tools, in: 45th IEEE Conference on Decision and Control, pp. 6678–6683.

Table 5: CPU time in [s], total time spent (TTS) in [h], total emissions (TE) of CO_2 in [kg], cost, and TTS and TE compared to the benchmark fixed-time controller (in %) within the entire 6-hour simulation time window of **case study 2**. For the abbreviations of the controllers: Opt. fixed-time is the optimized fixed-time controller; Conv. MPC is the conventional MPC controller; L-hori. MPC is the conventional MPC controller with a large prediction horizon; L-term MPC is the single-level long-term MPC controller. The notation '–' means that the item is not applicable to that controller. Note that the CPU time of the long-term MPC controller corresponds to a larger control sampling time than the other MPC controllers.

	Fixed-time	Responsive	OPAC	Opt. fixed-time	Conv. MPC	L-hori. MPC	L-term MPC	Bi-level MPC
CPU time [s]	–	–	–	–	105698	416035	20363	65432
CPU time per control step [s]	–	–	–	–	36.7	144.5	509.1	22.7
TTS [$\times 10^3$ hour]	188.830	160.993	159.611	167.606	179.748	159.527	169.357	159.578
TE(CO_2) [$\times 10^3$ kg]	2835.165	2610.805	2703.496	2655.158	2707.206	2586.102	2684.967	2598.886
Objective function value [$\times 10^3$]	203.006	174.047	173.129	180.882	193.284	172.458	182.782	172.572
Obj. value compared with Opt. fixed-time	+12.23%	-3.78%	-4.29%	–	+6.86%	-4.66%	+1.05%	-4.59%

Boggs, P.T., Tolle, J.W., 1995. Sequential quadratic programming. Acta numerica 4, 1–51.

Brandi, A., Ferrara, A., Sacone, S., Siri, S., Vivas, C., Rubio, F., 2017. Model predictive control with state estimation for freeway systems, in: American Control Conference (ACC), pp. 3536–3541.

Brdys, M., Grochowski, M., Gminski, T., Konarczak, K., Drewa, M., 2008. Hierarchical predictive control of integrated wastewater treatment systems. Control Engineering Practice 16, 751–767.

Camacho, E.F., Bordons, C., 1995. Model Predictive Control in Process Industry. Springer.

Di Cairano, S., Bäthge, T., Findeisen, R., 2019. Modular design for constrained control of actuator-plant cascades, in: 2019 American Control Conference (ACC), IEEE. pp. 1755–1760.

Dunham, W., Hencey, B., Girard, A.R., Kolmanovsky, I., 2019. Distributed model predictive control for more electric aircraft subsystems operating at multiple time scales. IEEE Transactions on Control Systems Technology 28, 2177–2190.

EC, 2021. Regulation (EU) 2021/1119 of the european parliament and of the council of 30 June 2021 establishing the framework for achieving climate neutrality and amending Regulations (EC) no 401/2009 and (EU) 2018/1999 ('European Climate Law').

Echeverría, L., Giménez-Nadal, J.I., Molina, J.A., 2022. Who uses green mobility? exploring profiles in developed countries. Transportation Research Part A: Policy and Practice 163, 247–265.

EEA, 2021. Air quality e-reporting.

Gartner, N.H., 1983. OPAC: A demand-responsive strategy for traffic signal control. Transportation Research Record Journal of the Transportation Research Board No. 906, 75–81.

Haddad, J., Ramezani, M., Geroliminis, N., 2013. Cooperative traffic control of a mixed network with two urban regions and a freeway. Transportation Research Part B: Methodological 54, 17–36.

Han, H.G., Fu, S.J., Sun, H.Y., Qiao, J.F., 2021. Hierarchical nonlinear model predictive control with multi-time-scale for wastewater treatment process. Journal of Process Control 108, 125–135.

Han, Y., Ramezani, M., Hegyi, A., Yuan, Y., Hoogendoorn, S., 2020. Hierarchical ramp metering in freeways: an aggregated modeling and control approach. Transportation Research Part C: Emerging Technologies 110, 1–19.

van Henten, E., Bontsema, J., 2009. Time-scale decomposition of an optimal control problem in greenhouse climate management. Control Engineering Practice 17, 88–96.

Jamshidnejad, A., Lin, S., Xi, Y., De Schutter, B., 2018a. Corrections to "Integrated urban traffic control for the reduction of travel delays and emissions". IEEE Transactions on Intelligent Transportation Systems 20, 1978–1983.

Jamshidnejad, A., Papamichail, I., Hellendoorn, H., Papageorgiou, M., De Schutter, B., 2016. Gradient-based model-predictive control for green urban mobility in traffic networks, in: 2016 IEEE 19th International Conference on Intelligent Transportation Systems, pp. 1077–1082.

Jamshidnejad, A., Papamichail, I., Papageorgiou, M., De Schutter, B., 2018b. Sustainable model-predictive control in urban traffic networks: Efficient solution based on general smoothening methods. IEEE Transactions on Control Systems Technology 26, 813–827.

Jin, X., Jiang, T., Mu, Y., Long, C., Li, X., Jia, H., Li, Z., 2019. Scheduling distributed energy resources and smart buildings of a microgrid via multi-time scale and model predictive control method. IET Renewable Power Generation 13, 816–833.

Kachroudi, S., Mammar, S., 2013. The effects of the control and prediction horizons on the urban traffic regulation, in: 13th International IEEE Conference on Intelligent Transportation Systems, IEEE.

Keyvan-Ekbatani, M., Gao, X., Gayah, V.V., Knoop, V.L., 2019. Traffic-responsive signals combined with perimeter control: investigating the benefits. Transportmetrica B: Transport Dynamics 7, 1402–1425.

Kong, Q.J., Xu, Y., Lin, S., Wen, D., Zhu, F., Liu, Y., 2013. UTN-model-based traffic flow prediction for parallel-transportation management systems. IEEE Transactions on Intelligent Transportation Systems 14, 1541–1547.

Lin, S., De Schutter, B., Xi, Y., Hellendoorn, H., 2011. Fast model predictive control for urban road networks via milp. IEEE Transactions on Intelligent Transportation Systems 12, 846–856.

Lin, S., De Schutter, B., Xi, Y., Hellendoorn, H., 2013. Integrated urban traffic control for the reduction of travel delays and emissions. IEEE Transactions on Intelligent Transportation Systems 14, 1609–1619.

Liu, D., Wu, J., Liu, H., Song, P., Wang, K., 2020. Multi-time scale energy management strategy of micro energy grid based on model predictive control, in: 2020 IEEE Sustainable Power and Energy Conference (iSPEC), IEEE. pp. 1511–1516.

Maciejowski, J., 2002. Predictive Control with Constraints. Prentice Hall.

Manolis, D., Pappa, T., Diakaki, C., Papamichail, I., Papageorgiou, M., 2018. Centralised versus decentralised signal control of large-scale urban road networks in real time: A simulation study. IET Intelligent Transport Systems 12, 891–900.

Morari, M., Lee, J.H., 1999. Model predictive control: Past, present, and future. Computers and Chemical Engineering 23, 667–682.

Oliveira, L.B.D., Camponogara, E., 2010. Multi-agent model predictive control of signaling split in urban traffic networks. Transportation Research Part C: Emerging Technologies 18, 120–139.

Outlook, I., 2017. Itf transport outlook 2017.

Pappas, G.J., Lafferriere, G., Sastry, S., 2000. Hierarchically consistent control systems. IEEE Transactions on Automatic Control 45, 1144–1160.

Rawlings, J.B., Mayne, D.Q., 2009. Model Predictive Control: Theory and Design. Nob Hill Publishing.

Richter, S., Jones, C.N., Morari, M., 2012. Computational complexity certification for real-time mpc with input constraints based on the fast gradient method. IEEE Transactions on Automatic Control 57, 1391–1403.

Roncoli, C., Papamichail, I., Papageorgiou, M., 2016. Hierarchical model predictive control for multi-lane motorways in presence of vehicle automation and communication systems. Transportation Research Part C: Emerging Technologies 62, 117–132.

Scattolini, R., 2009. Architectures for distributed and hierarchical model predictive control–a review. Journal of Process Control 19, 723–731.

De Schutter, B., 2014. Model predictive traffic control for green mobility, in: 2014 European Control Conference, pp. 2260–2263.

Siri, S., Pasquale, C., Sacone, S., Ferrara, A., 2021. Freeway traffic control: A survey. Automatica 130, 109655.

Skaf, J., Boyd, S., Zeevi, A., 2010. Shrinking-horizon dynamic programming. International Journal of Robust and Nonlinear Control 20, 1993–2002.

Su, Z., Jamshidi, A., Núñez, A., Baldi, S., De Schutter, B., 2017. Multi-level condition-based maintenance planning for railway infrastructures–a scenario-based chance-constrained approach. Transportation Research Part C: Emerging Technologies 84, 92–123.

Su, Z., Jamshidi, A., Núñez, A., Baldi, S., De Schutter, B., 2019. Integrated condition-based track maintenance planning and crew scheduling of rail-

way networks. Transportation Research Part C: Emerging Technologies 105, 359–384.

Tettamanti, T., 2013. Advanced Methods for Measurement and Control in Urban Road Traffic Networks. Ph.D. thesis. Budapest University of Technology and Economics.

Tettamanti, T., Luspay, T., Kulcsar, B., Péni, T., Varga, I., 2013. Robust control for urban road traffic networks. IEEE Transactions on Intelligent Transportation Systems 15, 385–398.

Tettamanti, T., Varga, I., Kulcsár, B., Bokor, J., 2008. Model predictive control in urban traffic network management, in: 2008 16th Mediterranean Conference on Control and Automation, IEEE. pp. 1538–1543.

UNEP, U., 2020. Emissions gap report 2020. UN environment programme .

Varaiya, P., 1993. Smart cars on smart roads: problems of control. IEEE Transactions on Automatic Control 38, 195–207.

van de Weg, G.S., Vu, H.L., Hegyi, A., Hoogendoorn, S.P., 2018. A hierarchical control framework for coordination of intersection signal timings in all traffic regimes. IEEE Transactions on Intelligent Transportation Systems 20, 1815–1827.

Wu, N., Li, D., Xi, Y., De Schutter, B., 2020. Distributed event-triggered model predictive control for urban traffic lights. IEEE Transactions on Intelligent Transportation Systems 22, 4975–4985.

Ye, B.L., Wu, W., Ruan, K., Li, L., Chen, T., Gao, H., Chen, Y., 2019. A survey of model predictive control methods for traffic signal control. IEEE/CAA Journal of Automatica Sinica 6, 623–640.

Zegeye, S., De Schutter, B., Hellendoorn, J., Breunesse, E., Hegyi, A., 2013. Integrated macroscopic traffic flow, emission, and fuel consumption model for control purposes. Transportation Research Part C: Emerging Technologies 31, 158–171.